Caged and Uncaged Ruthenium(II)-Polypyridine Complexes. Comparative Study of the Photochemical, Photophysical, and Electrochemical Properties

Francesco Barigelletti,[1a] Luisa De Cola,[1a] Vincenzo Balzani,*[,1a,b] Peter Belser,[1c] Alex von Zelewsky,[1c] Fritz Vögtle,[1d] Frank Ebmeyer,[1d] and Smaragda Grammenudi[1d]

Contribution from the Istituto FRAE—CNR and Dipartimento di Chimica "G. Ciamician" dell' Università, Bologna, Italy, Institute of Inorganic Chemistry, University of Fribourg, Fribourg, Switzerland, and Institut für Organische Chemie und Biochemie, University of Bonn, Bonn, FRG.
Received October 24, 1988

Abstract: The absorption spectra, emission spectra (from 90 to 350 K), luminescence lifetimes (from 90 to 350 K), luminescence quantum yields, luminescence quenching by dioxygen, photochemical behavior, and redox potentials of a caged (**4**) and a hemicaged (**3**) Ru(II)-polypyridine complex have been studied and compared with those of the parent compounds $Ru(bpy)_3^{2+}$ (**1**) and $Ru(5,5'-(EtO_2C)_2\text{-}bpy)_3^{2+}$ (**2**) (bpy = 2,2'-bipyridine). The absorption band in the visible and the emission band of **4** are quite close in energy to the corresponding bands of **1**, whereas those of **3** and **2** are red shifted. The oxidation and reduction processes of **3** and **4** take place at more positive potentials than those of **1**. A linear correlation between the spectroscopic and electrochemical energies is observed for the four complexes. The luminescence lifetimes of **2** (0.57 μs) and **3** (1.9 μs) are shorter than those of **1** (4.8 μs) and **4** (4.8 μs) in nitrile rigid matrix at 90 K and are much more affected by the melting of the matrix (110–150 K). For $T > 150$ K (i.e., in fluid solution), the luminescence lifetimes of **2** and **3** (0.09 and 0.45 μs) do not change up to 350 K, in contrast with the well-known behavior of **1**, where a radiationless activated process with high-frequency factor ($A \sim 10^{14}$ s^{-1}) and large activation energy ($\Delta E \sim 4000$ cm^{-1}) reduces the excited-state lifetime to 0.80 μs at room temperature. The caged complex **4** exhibits a less important radiationless activated process ($A \sim 10^{10}$ s^{-1}, $\Delta E \sim 2700$ cm^{-1}) and maintains a longer lifetime (1.7 μs) at room temperature. In CH_2Cl_2 solution containing 0.01 M Cl^-, $Ru(bpy)_3(PF_6)_2$ undergoes a photodecomposition reaction with $\Phi_p = 0.017$, whereas the PF_6^- salts of **2**–**4** are photoinert ($\Phi_p \leq 10^{-6}$ for **4**). The rate constant for the dioxygen quenching of the luminescent excited state of **4** is ca. 5 times smaller than that of **1**. A comparative discussion of the properties of the four complexes is presented. The cage complex **4** exhibits all the properties that make **1** a widely used photosensitizer, with the additional advantages of a longer excited-state lifetime at room temperature in fluid solution and a 10^4 times higher stability toward ligand photodissociation.

In the past 10 years $Ru(bpy)_3^{2+}$ (bpy = 2,2'-bipyridine) and a number of other Ru(II)-polypyridine complexes have been the object of many investigations because of their ability to luminesce and to play the role of mediators (sensitizers) in photochemical and chemiluminescent processes.[2-5] Comparison with the properties needed for ideal luminophores and photosensitizers[6,7] shows that the main drawbacks of $Ru(bpy)_3^{2+}$ are (i) the relatively fast radiationless decay of its lowest excited state (which is that responsible for luminescence and for energy and electron-transfer processes) and (ii) the occurrence of ligand photodissociation processes. Several attempts have been performed to remedy these drawbacks by manipulation of the ligand coordination sphere, i.e., introducing substituents on the bpy rings and/or replacing bpy with other polypyridine ligands.[2-15] These studies have shown that it is indeed possible to change gradually several ground- and excited-state properties over a broad range of values, but generally the improvement of a specific property compromises other properties. For example, a higher photochemical stability is usually accompanied by a shorter excited-state lifetime.

It is generally agreed[2-5,16,17] that the ligand photodissociation reaction of $Ru(bpy)_3^{2+}$ proceeds via a thermally activated radiationless transition from the luminescent triplet metal-to-ligand charge-transfer (^{3}MLCT) level to a distorted triplet metal-centered (^{3}MC) level, with subsequent cleavage of one Ru–N bond. The commonly used strategy to improve the photochemical stability is to increase the energy gap between the ^{3}MC and ^{3}MLCT levels so as to prevent or at least reduce the population of the former. Since the energy of the ^{3}MC level cannot be increased (actually, the ligand field strength generally decreases when bpy is replaced by other polypyridine ligands), a larger energy gap between ^{3}MC and ^{3}MLCT states can only be obtained by decreasing the energy of the ^{3}MLCT level. This, however, increases the rate of the temperature-independent nonradiative decay from ^{3}MLCT directly to the ground state, with a consequent decrease of the excited-state lifetime and of the luminescence quantum yield.

An alternative way to prevent ligand photodissociation is to link the ligands together so as to make a cage structure around the metal.[7,18] This approach, first used by Sargeson et al.[19] to stabilize Co(II) complexes, is indeed very effective and also offers additional advantages. The spectroscopic properties and the temperature-independent decay processes are not affected by caging because the first coordination sphere of the metal (and thus, the energy level diagram near the equilibrium nuclear configuration) does not change.[18] Furthermore, a cage structure can confer more

(1) (a) Istituto FRAE—CNR, Bologna. (b) University of Bologna. (c) University of Fribourg. (d) University of Bonn.
(2) Juris, A.; Balzani, V.; Barigelletti, F.; Campagna, S.; Belser, P.; von Zelewsky, A. *Coord. Chem. Rev.* **1988**, *84*, 85.
(3) Krause, R. A. *Struct. Bonding* **1987**, *67*, 1.
(4) Kalyanasundaram, K. *Coord. Chem. Rev.* **1982**, *46*, 159.
(5) Seddon, E. A.; Seddon, K. R. *The Chemistry of Ruthenium*; Elsevier: Amsterdam, The Netherlands, 1984; Chapter 15.
(6) Balzani, V.; Juris, A.; Scandola, F. In *Homogeneous and Heterogeneous Photocatalysis*; Pelizzetti, E., Serpone, N.; Eds.; Reidel: Dordrecht, The Netherlands, 1986; p 1.
(7) Balzani, V. *Gazz. Chim. Ital.* In press.
(8) Allen, G. H.; White, R. P.; Rillema, D. P.; Meyer, T. J. *J. Am. Chem. Soc.* **1984**, *106*, 2613.
(9) Caspar, J. V.; Meyer, T. J. *Inorg. Chem.* **1983**, *22*, 2444.
(10) Henderson, L. J., Jr.; Cherry, W. R. *J. Photochem.* **1985**, *28*, 143.
(11) Wacholtz, W. M.; Auerbach, R. A.; Schmehl, R. H.; Ollino, M.; Cherry, W. R. *Inorg. Chem.* **1985**, *24*, 1758.
(12) Wacholtz, W. F.; Auerbach, R. A.; Schmehl, R. H. *Inorg. Chem.* **1986**, *25*, 227.
(13) Barigelletti, F.; Juris, A.; Balzani, V.; Belser, P.; von Zelewsky, A. *Inorg. Chem.* **1983**, *22*, 3335.
(14) De Cola, L.; Barigelletti, F.; Cook, M. J. *Helv. Chim. Acta* **1988**, *71*, 733.
(15) Balzani, V.; Juris, A.; Barigelletti, F.; Belser, P.; von Zelewsky, A. *Sci. Pap. Inst. Phys. Chem. Res. (Jpn.)* **1984**, *78*, 78.
(16) Van Houten, J.; Watts, R. J. *Inorg. Chem.* **1978**, *17*, 3381.
(17) Durham, B.; Caspar, J. V.; Nagle, J. K.; Meyer, T. J. *J. Am. Chem. Soc.* **1982**, *104*, 4803.
(18) Balzani, V.; Sabbatini, N.; Scandola, F. *Chem. Rev.* **1986**, *86*, 319.
(19) Sargeson, A. M. *Chem. Br.* **1979**, *15*, 23; *Pure Appl. Chem.* **1984**, *56*, 1603.

0002-7863/89/1511-4662$01.50/0

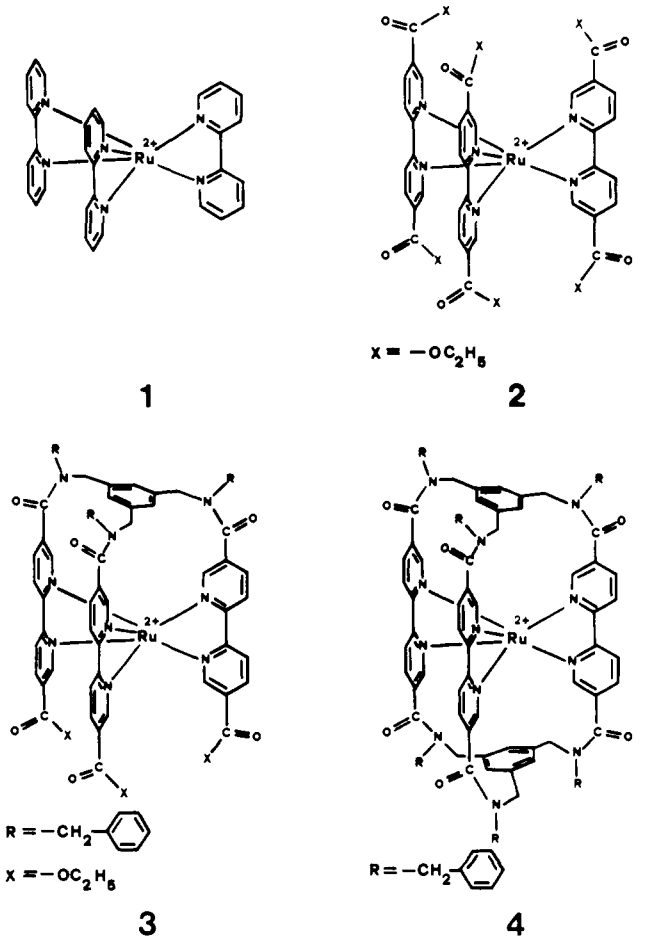

Figure 1. Schematic representation of the complexes studied: Ru(bpy)$_3^{2+}$ (1), Ru(5,5′-(EtO$_2$C)$_2$-bpy)$_3^{2+}$ (2), hemicaged complex (3), and cage complex (4).

rigidity to the molecule, thereby reducing the rate of thermally activated radiationless decay processes.

One can thus expect that suitable caging of the Ru(bpy)$_3^{2+}$ structure can prevent ligand photodissociation and also increase the lifetime of ^{3}MLCT and the luminescence quantum yield. Inspection of CPK molecular models shows that the cryptand bpy ligand used for lanthanide ions[20] is not suitable to provide the right octahedral coordination site for Ru^{2+}. Therefore one could expect that for such Ru(II) cryptate the short-lived ^{3}MC level has to be lower than the ^{3}MLCT level, thereby offering a fast radiationless decay route. This seems to be confirmed by a recent report by Dürr et al.,[21] who claim to have prepared such a cryptate. By contrast, the spacered close-cage ligand recently synthesized in one of our laboratories[22] was expected to be flexible enough to provide an octahedral site quite similar to that present in Ru(bpy)$_3^{2+}$.

Following the above concepts, we have recently synthesized and characterized the caged[23] and hemicaged Ru(II)–polypyridine complexes **4** and **3** (Figure 1). In this paper we report the results[24] of a detailed investigation on the photochemical, photophysical, and electrochemical properties of such complexes and a comparative discussion of the results obtained with those previously available for the Ru(bpy)$_3^{2+}$ [2,5] (**1**) and Ru(5,5′-(EtO$_2$C)$_2$-bpy)$_3^{2+}$ [25-27] (**2**) parent compounds.

Experimental Section

All the employed solvents were of the best grade commercially available. $RuCl_3{\cdot}3H_2O$ and NH_4PF_6 were purchased from Johnson-Mattey and Fluka, respectively, and used without further purification. Ru(bpy)$_3$(PF$_6$)$_2$ was available from previous studies in our laboratories. **2** was prepared by a method previously reported.[27] The ligand used for the synthesis of complex **3** was prepared by Vögtle and co-workers.[22] **3** was prepared by heating at 120 °C equimolar amounts of $RuCl_3{\cdot}3H_2O$ and of the ligand in ethylene glycol for 5 h. The dark orange solution was evaporated under vacuum and the residue dissolved in H_2O. Addition of a saturated aqueous NH_4PF_6 solution caused the precipitation of the complex salt. The solid was collected by vacuum filtration, air-dried, and then purified by chromatography on neutral alumina eluted with acetone containing 1% H_2O. The complex was then recrystallized from acetonitrile/ether. **4** was prepared as previously reported.[23] Details on the synthesis and characterization of **3** and **4** will be given elsewhere.[29]

The absorption spectra were recorded with a Perkin-Elmer λ5 spectrophotometer. Uncorrected emission spectra were obtained with a Perkin-Elmer 44B spectrofluorometer equipped with a Hamamatsu R928 tube. Corrected emission spectra were obtained with a Perkin-Elmer LS5 spectrofluorometer using a calibrated light source. Emission quantum yields were obtained with the optically diluted method using Ru(bpy)$_3^{2+}$ in deaerated CH_3CN (AN) solution as a standard (Φ_{em} = 0.062).[30] The estimated uncertainty is ±20%.

The emission lifetimes were measured by a modified Applied Photophysics single-photon equipment.[13] The temperature-dependence experiments were carried out in a mixture of freshly distilled propionitrile/butyronitrile (4:5 v/v) (nitrile). A dilute solution of each complex was sealed under vacuum in a 1-cm quartz cell after repeated freeze–pump–thaw cycles. The cell was placed inside a Thor C600 nitrogen flow cryostat, equipped with a Thor 3030 temperature controller. The absolute error on the temperature is estimated to be ±2 K. In order to minimize solvent dynamic effects in the melting region of the solvent,[31] the emission decay was always monitored at the maximum of the emission band by using interference filters. The single-exponential analysis was performed with nonlinear programs,[32] and the quality of the fit was assessed by the χ^2 value close to unity and by a regular distribution of the residuals along the time axis. The experimental error on the lifetime is estimated to be ≤8%. Standard iterative nonlinear programs[32] were also employed to extract the parameters for the temperature dependence of the lifetime.

The photochemical experiments were carried out on PF_6^- salts at room temperature in air-equilibrated CH_2Cl_2 solutions containing 0.01 M Cl^- as benzyl(triethyl)ammonium chloride. Excitation was performed with a tungsten halogen lamp using a Balzers interference filter to isolate a band centered at 462 nm. The incident light intensity (1.8×10^{-6} N$h\nu$/min) was measured with an Aberchrome actinometer.[33] The irradiated solution was contained in a 3-mL spectrophotometric cell housed in a thermostated holder. For Ru(bpy)$_3^{2+}$ and the cage complex **4**, comparative photostability experiments were also performed using the polychromatic light of a tungsten halogen lamp. A neutral density filter (transmittance = 1%) was used to reduce the light intensity for irradiation of Ru(bpy)$_3^{2+}$ solutions. The occurrence of photoreactions was followed by spectrophotometric analysis in the visible region. The quantum yield for Ru(bpy)$_3^{2+}$ photodissociation was measured from the change in absorbance at 452 nm and the extinction coefficients of the reactant and product [Ru(bpy)$_2$Cl$_2$].[34] For the other complexes, the estimated limiting quantum yields were based on the assumption that the reaction product had a spectrum similar to that of Ru(bpy)$_2$Cl$_2$.

(20) Rodriguez-Ubis, J. C.; Alpha, B.; Plancherel, D.; Lehn, J. M. *Helv. Chim. Acta* **1984**, *67*, 2264. Lehn, J. M. In *Supramolecular Photochemistry*; Balzani, V., Ed.; Reidel: Dordrecht, The Netherlands, 1987; p 29.
(21) Dürr, H.; Zengerle, K.; Trierweiler, H.-P. *Z. Naturforsch.* **1988**, *43B*, 361.
(22) (a) Grammenudi, S.; Vögtle, F. *Angew. Chem., Int. Ed. Engl.* **1986**, *25*, 1122. (b) Grammenudi, S.; Franke, M.; Vögtle, F.; Steckman, E. Y. *J. Inclusion Phenom.* **1987**, *5*, 695.
(23) Belser, P.; De Cola, L.; von Zelewsky, A. *J. Chem. Soc., Chem. Commun.* **1988**, 1057.
(24) For a preliminary communication, see: De Cola, L.; Barigelletti, F.; Balzani, V.; Belser, P.; von Zelewsky, A.; Vögtle, F.; Ebmeyer, F.; Grammenudi, S. *J. Am. Chem. Soc.* **1988**, *110*, 7210.
(25) Monserrat, K.; Foreman, T. K.; Grätzel, M.; Whitten, D. J. *J. Am. Chem. Soc.* **1981**, *103*, 6667.
(26) Oshawa, Y.; Whangbo, M.-H.; Hanck, K. W.; De Armond, K. M. *Inorg. Chem.* **1984**, *23*, 3426.
(27) Elliot, M. C.; Hershenhart, E. J. *J. Am. Chem. Soc.* **1982**, *104*, 7519.
(28) Gas, B.; Klima, J.; Zalis, S.; Vlček, A. A. *J. Electroanal. Chem.* **1987**, *222*, 161.
(29) De Cola, L.; Belser, P., to be published.
(30) Calvert, J. M.; Caspar, J. V.; Binstead, R. A.; Westmoreland, T. D.; Meyer, T. J. *J. Am. Chem. Soc.* **1982**, *104*, 6620.
(31) Kim, H.-B.; Kitamura, N.; Tazuke, S. *Chem. Phys. Lett.* **1988**, *143*, 77.
(32) Bevington, P. R. *Data Reduction and Error Analysis for Physical Sciences*, McGraw Hill: New York, 1969.
(33) Heller, H. G.; Langan, J. R. *J. Chem. Soc., Perkin. Trans. 2* **1981**, 341.
(34) Gleria, M.; Minto, F.; Beggiato, G.; Bortolus, P. *J. Chem. Soc., Chem. Commun.* **1978**, 285.

Table I. Spectroscopic, Photochemical, and Photophysical Properties

	absorption[a] (298 K)		emission[b]					
			90 K		298 K			photochemistry[c]
complex	λ_{max}, nm	$\epsilon^d \times 10^{-3}$	λ_{max}, nm	τ, μs	λ_{max}, nm	τ, μs	$\Phi_{em} \times 10^{2e}$	(298 K) Φ_p
1	452	13.0	582	4.8	615	0.80	6.2	0.017[f]
2	500	10.0	657	0.53	665	0.09	0.6	$<10^{-5}$
3	477	9.5	620	1.9	640	0.45	2.7	$<10^{-5}$
4	455	10.4	597	4.8	612	1.70	8.7	$<10^{-6}$

[a] CH_3CN solution. [b] Deaerated propionitrile/butyronitrile solution, unless otherwise stated. Estimated uncertainties: lifetime, ≤8%; quantum yield, ±20%. [c] For PF_6^- salts, in CH_2Cl_2 solution containing 0.01 M Cl^-. [d] Extinction coefficient, cm^{-1} M^{-1}. [e] Deaerated CH_3CN solution. [f] Estimated uncertainty, ±0.004.

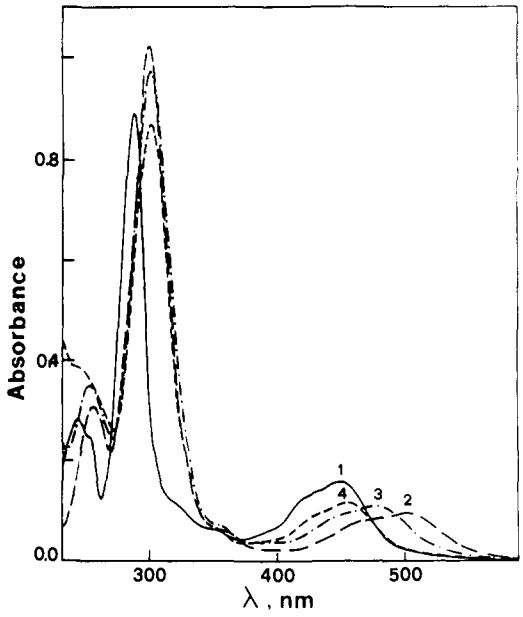

Figure 2. Absorption spectra in AN solution at room temperature. The complexes are labeled as in Figure 1.

Electrochemical measurements were carried out at room temperature (~25 °C) by using a Metrohm E/506 Polarecord, a Metrohm E/612 VA scanner, and a Hewlett-Packard 7044 x-y recorder. Cyclic voltammograms were obtained in AN solution by using a microcell equipped with a stationary platinum disk electrode, a platinum wire counter electrode, and a silver wire reference electrode with tetrabutylammonium perchlorate (TBAP) as supporting electrolyte. For all complexes, except **4**, a normal cell equipped with a SCE was also used, obtaining the same results. In all cases $Ru(bpy)_3^{2+}$ was used as an internal standard, taking its oxidation potential equal to +1.260 V vs SCE.[35,36] The electrochemical window examined was between +2.0 and −2.0 V. Scanning speed was usually 200 mV s^{-1}. All the reported values are vs SCE. Half-wave potentials were calculated as an average of the cathodic and anodic peak potentials. The separation between cathodic and anodic peaks and the relative intensities of the cathodic and anodic currents were taken as criteria for reversibility.

Results

The absorption spectra in acetonitrile solutions are shown in Figure 2. The luminescence spectra in nitrile solutions at 90 K are shown in Figure 3. The wavelengths and extinction coefficients of the absorption maxima in the visible region at 298 K, the wavelengths of the emission maxima at 90 and 298 K, the luminescence lifetimes at 90 and 298 K, and the quantum yields of luminescence at 298 K are shown in Table I. The luminescence spectra and lifetimes were examined in the entire temperature range between 90 and 350 K and the results obtained are summarized by the plots of Figures 4–6.

The luminescence intensities and lifetimes in acetonitrile solution at room temperature were quenched in parallel by dioxygen. The values for $k_q[O_2]$ were 4.7×10^6 and 1.0×10^6 s^{-1} for **1** and **4**, respectively.

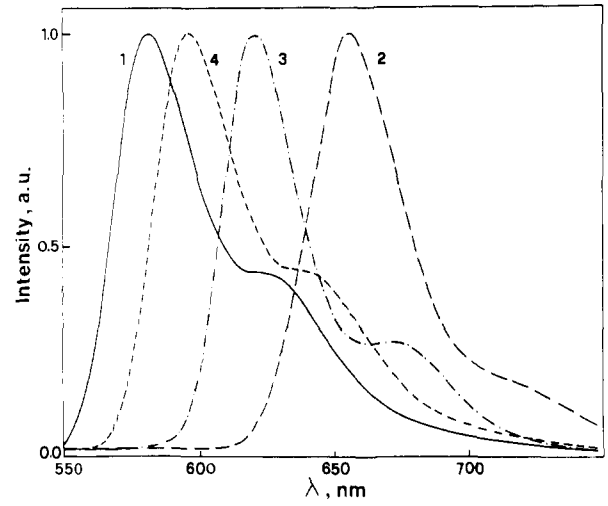

Figure 3. Luminescence spectra in a proprionitrile/butyronitrile (4:5, v/v) rigid matrix at 90 K. The complexes are labeled as in Figure 1.

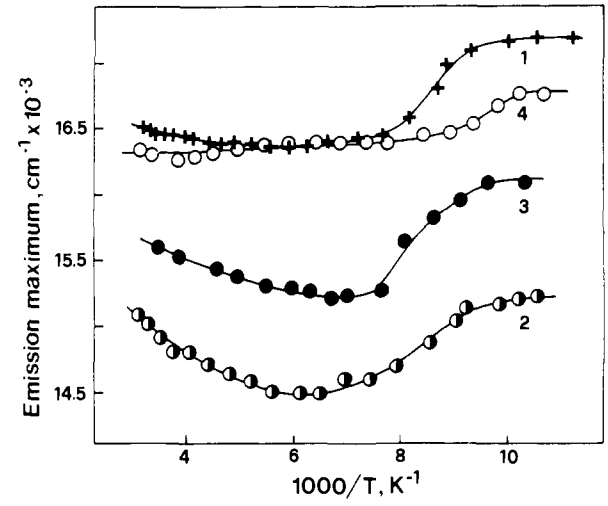

Figure 4. Shift of the maximum of the luminescence band with temperature. The complexes are labeled as in Figure 1.

In CH_2Cl_2 solutions containing 0.01 M Cl^-, irradiation with 462-nm light (see Experimental Section) caused quite large spectral changes in a few minutes for $Ru(bpy)_3(PF_6)_2$. In agreement with previous reports,[2-5] the intensity of the band at 452 nm decreased and a lower intensity band appeared at longer wavelength (λ_{max} = 552 nm), as expected for the formation of $Ru(bpy)_2Cl_2$.[34] Under our experimental conditions, the quantum yield of $Ru(bpy)_3^{2+}$ disappearance was 0.017 ± 0.004. Under the same experimental conditions, no spectral change was observed for **2**–**4**, even after 84 h of irradiation, showing that the upper limit for the photodecomposition quantum yield of those complexes is lower than 10^{-5}. In an attempt to obtain a more precise limiting value for the quantum yield of photodecomposition of the cage complex **4**, we have taken advantage of the similarity of the

(35) Juris, A.; Balzani, V.; Belser, P.; von Zelewsky, A. *Helv. Chim. Acta* **1981**, *64*, 2175.
(36) Sutin, N.; Creutz, C. *Adv. Chem. Ser.* **1978**, *168*, 1. Lin, C. T.; Boettcher, W.; Chou, M.; Creutz, C.; Sutin, N. *J. Am. Chem. Soc.* **1976**, *98*, 6536.

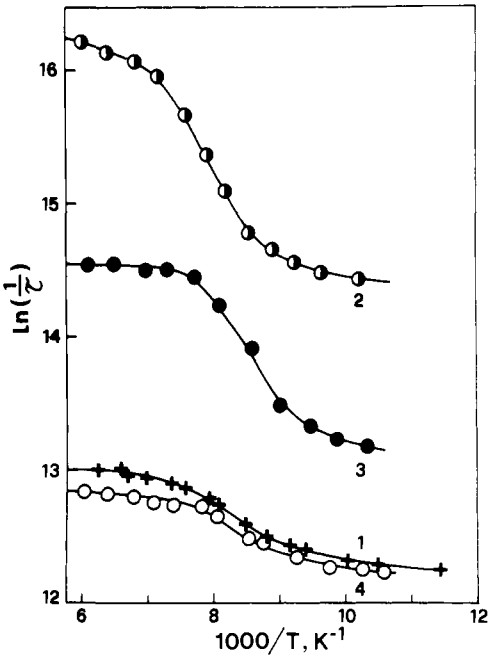

Figure 5. Temperature dependence of the luminescence lifetime in the low-temperature region (90–170 K). The melting of the solvent matrix occurs approximately in the temperature range 110–140 K. The complexes are labeled as in Figure 1.

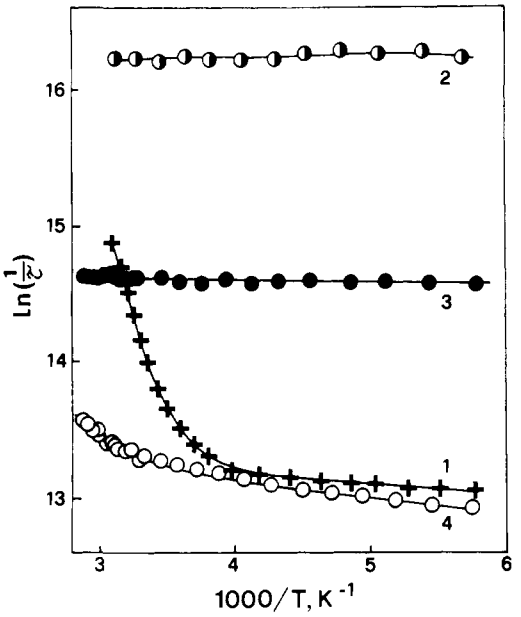

Figure 6. Temperature dependence of the luminescence lifetime in the high-temperature region (170–350 K). The complexes are labeled as in Figure 1.

absorption bands of $Ru(bpy)_3^{2+}$ and **4** and we have irradiated solutions of the two complexes, exhibiting the same absorbance at 452 nm, with the full light of a tungsten halogen lamp (see Experimental Section). From those experiments, we estimated that the quantum yield of photodecomposition of **4** has to be at least 10^4 times smaller than that of $Ru(bpy)_3^{2+}$. It should be pointed out that the measurement or even the evaluation of very small quantum yields is usually a difficult task. Under our experimental conditions, for example, the very high light intensity and the very long irradiation time could have caused some minor photoreaction of the CH_2Cl_2 solvent or of an impurity that could have induced some photodegradation reaction of **4** not related to its photodissociation. Thus, the photostability of the cage complex toward metal–ligand photodissociation may even be much higher than indicated by the reported limiting value of Φ_p. The relative photostability experiment could not be performed with **2** and with

Table II. Electrochemical Data

complex	redox potentials,[a] V			
	3+/2+	2+/1+	1+/0	0/1−
1	+1.26	−1.35	−1.54	−1.79
2[b]	+1.55	−0.74	−0.86	−1.03
3	+1.54	−0.86	−0.99	−1.17
4	+1.55[c]	−1.01	−1.20	−1.38

[a] CH_3CN solution, room temperature. The reported values are the average of the anodic and cathodic CV peaks. The processes are reversible except otherwise indicated. [b] Other reversible waves were observed at −1.40, −1.59, and −1.82 V. [c] Irreversible ($\Delta V \sim 170$ mV), see text.

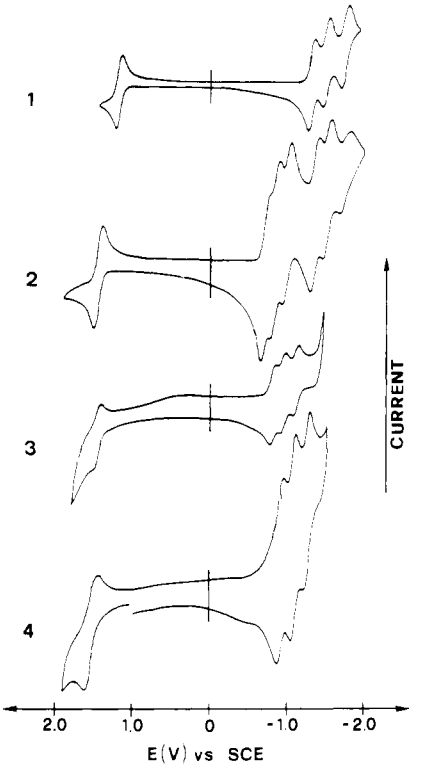

Figure 7. Cyclic voltammograms in AN solution at sweep rate 200 mV/s. The complexes are labeled as in Figure 1.

3 because their absorption spectra in the visible region are substantially different from that of $Ru(bpy)_3^{2+}$ (Figure 2), thereby making a comparison of results on irradiation with the full light of the lamp impossible.

The electrochemical measurements showed that each complex undergoes one oxidation and several reduction processes. Figure 7 shows the cyclic voltammograms and Table II collects the potential values. The observed waves are nearly reversible ($\Delta E_p \sim 80$ mV) with the exception of the oxidation wave of **4** ($\Delta E_p \sim 170$ mV). The cyclic voltammograms indicated that the oxidation product of **4** is chemically stable and that the electrochemical irreversibility may originate from a slow electron-transfer rate.

Discussion

Absorption Spectra. The absorption spectrum of $Ru(bpy)_3^{2+}$ (Figure 2) has been discussed in detail by many authors.[2-5,37-39] The bands at 185 nm (not shown in the figure) and 285 nm have been assigned to ligand-centered (LC) $\pi \rightarrow \pi^*$ transitions in the bpy ligands. The two remaining intense bands at 240 and 450 nm have been assigned to metal-to-ligand charge-transfer (MLCT) $d \rightarrow \pi^*$ transitions. The two shoulders between 300 and 350 nm are likely due to metal-centered (MC) $d \rightarrow d$ transitions. For

(37) Crosby, G. A. *Acc. Chem. Res.* **1975**, *8*, 231.
(38) Kemp, T. J. *Prog. React. Kinet.* **1980**, *10*, 301.
(39) Krausz, E. *Comments Inorg. Chem.* **1988**, *7*, 139.

the purpose of our discussion, the most interesting band is that in the visible, assigned to the lowest energy singlet MLCT excited state. As one can see from Figure 2, in the case of **2** this band is considerably red shifted compared to that of $Ru(bpy)_3^{2+}$ because the ester substituents are electron-withdrawing groups which increase the electronic affinity of the bpy ligands.[40,41] On caging, however, the ester groups are replaced by amide groups which are less electron withdrawing.[40] As seen in molecular models, the CO groups connected with the cap assume an approximately orthogonal orientation with respect to the bpy rings, reducing thereby the electronic delocalization. For these reasons, the MLCT band of the hemicaged complex **3** is blue shifted compared to that of **2** and the band of the closed cage complex **4** is further blue shifted. Actually, the band of **4** is very close in energy to that of $Ru(bpy)_3^{2+}$, showing that the (inner) chromophoric group of the cage complex is quite similar to $Ru(bpy)_3^{2+}$. The smaller extinction coefficient of the MLCT band of the caged complex compared with that of $Ru(bpy)_3^{2+}$ may reflect a slightly different coordination geometry in the two complexes. From Figure 2 one can also note that all the complexes exhibit a MC band at the same wavelength (~355 nm), indicating a quite similar ligand field strength. All the complexes also exhibit the strong LC bpy absorption in the 300-nm region, indicating again a substantial similarity between bridged and unbridged bpy ligands.

Luminescence Spectra. The luminescence of $Ru(bpy)_3^{2+}$ has been the object of extensive investigations,[2-5,37-39,42,43] and although there are still different views on important details, there is no doubt about its ^{3}MLCT origin. With only a few exceptions[2] this is also the case for the other Ru(II)–polypyridine complexes. The luminescence of **2** is red shifted compared to that of $Ru(bpy)_3^{2+}$ (Figure 2) as expected because of the lower energy of ^{1}MLCT. The luminescent spectra of **3** and **4** (Figure 2) are quite similar in shape to those of the parent $Ru(bpy)_3^{2+}$ and **2** complexes, and the energies of the emission bands of the four complexes correlate well with the energies of the MLCT absorption band in the visible. This shows that the emission of **3** and **4** is a regular ^{3}MLCT luminescence and confirms that the chromophoric group of the cage complex **4** is quite similar to that of $Ru(bpy)_3^{2+}$. These conclusions are reinforced by examination of lifetime data (Table I), which will be discussed in more detail later on. It can be noted, in particular, that at low temperature (90 K) the emission lifetimes of **3** and **4** are in the microsecond time range as expected for ^{3}MLCT luminescence of Ru(II)–polypyridine complexes and that the lifetime of **4** and $Ru(bpy)_3^{2+}$ are the same.

Correlation between Spectroscopic and Electrochemical Data. It is well-known[44,45] that $Ru(LL)_3^{2+}$ polypyridine complexes undergo an oxidation process centered on the metal and a series of three reduction waves corresponding to successive one-electron reduction of the three bidentate ligands. The hemicaged **3** and caged **4** complexes follow this general behavior (Figure 7, Table II). All the observed redox processes are reversible with the exception of the oxidation of **4**, which yields a chemically stable species but exhibits a somewhat irreversible kinetic character. We believe that the reason for the slow electron-transfer rate for the oxidation of **4** is related to the fact that the metal is buried in the ligand cage and therefore it cannot approach the electrode at a sufficiently close distance.

Because the orbitals involved in the first oxidation and reduction processes of Ru(II)–polypyridine complexes are the same as those involved in the spectroscopic transitions responsible for the lowest energy ^{3}MLCT and ^{1}MLCT excited states, a linear relationship is usually observed between the energies of the emission and absorption bands and $\Delta E_{1/2}$, defined as

$$\Delta E_{1/2} = e[E_{1/2}(ox) - E_{1/2}(red)] \quad (1)$$

where $E_{1/2}(ox)$ and $E_{1/2}(red)$ are the first oxidation and the first reduction potentials.[46-49] As shown by Figure 8, such a relationship holds for the complexes studied in this paper. The oxidation potential of **2** is more positive than that of $Ru(bpy)_3^{2+}$ (Table II) because of the withdrawing effect of the ester substituents.[40] At first sight it is surprising to see that the oxidation potential of the cage complex **4**, where the ester substituents have been replaced by the less withdrawing amide substituents, is more positive than that of $Ru(bpy)_3^{2+}$ and practically equal to that of **2**. This effect could be due to several factors. A partial contribution might come from differences in the solvation energies of the oxidized and reduced forms. $Ru(bpy)_3^{2+}$ is smaller and has sites where solvent molecules can easily penetrate, while **4** is larger and its central metal is better shielded from solvent interactions. Different solvation effects appear also from the temperature dependence of the emission energies and lifetimes, as will be discussed in detail in the next section. However, solvent effects are expected to cause deviations in the plots of Figure 8, which does not seem to be the case. Therefore, the main effect should be electronic in origin, perhaps related to strains on the metal–ligand bonds created by the cage structure. The oxidation potential of **3** is in line with those of the **2** and **4** parents.

The ligands of **2** are easier to reduce than bpy because of the presence of the ester groups.[26,27] This is the reason why the three reduction waves (each related to the one-electron reduction of a ligand) occur at noticeably less negative potentials for **2** than for

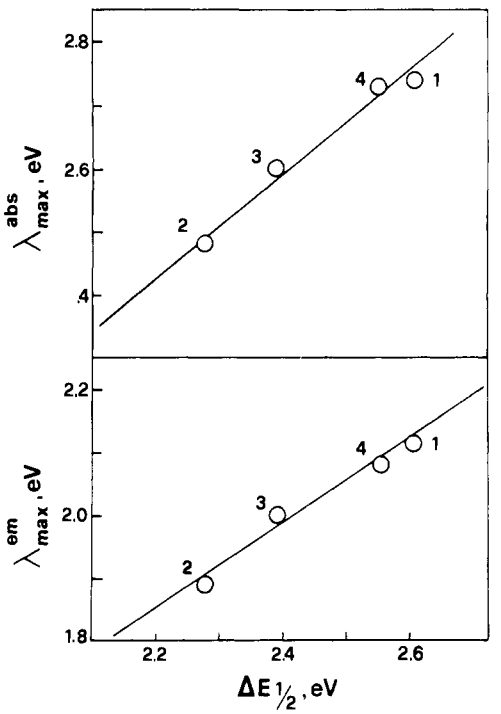

Figure 8. Correlations of the energies of absorption at room temperature (top) and emission at 90 K (bottom) maxima with the redox energy, $\Delta E_{1/2}$. The complexes are labeled as in Figure 1. Linear regression parameters: slope = 0.78, r = 0.99 (top); slope = 0.66, r = 0.98 (bottom).

(40) The σ_m Hammett constants for the acetamido and carbomethoxy groups are 0.14 and 0.35, respectively; see: Carey, F. A.; Sundberg, R. J. *Advanced Organic Chemistry*; Plenum Press: New York, 1984; Vol. 1, Chapter 4.

(41) Skarda, V.; Cook, M. J.; Lewis, A. P.; McAuliffe, G. S. G.; Thomson, A. J. *J. Chem. Soc., Perkin Trans. 2* **1984**, 1309.

(42) Myrick, M. L.; Blakley, R. L.; De Armond, M. K.; Arthur, M. L. *J. Am. Chem. Soc.* **1988**, *110*, 1325.

(43) Gallhuber, E.; Hensler, G.; Yersin, H. In *Photochemistry and Photophysics of Coordination Compounds*; Yersin, H., Vogler, A., Eds.; Springer Verlag: Berlin, 1987; p 93, and references therein.

(44) Vlček, A. A. *Coord. Chem. Rev.* **1982**, *43*, 39.

(45) De Armond, M. K.; Carlin, C. M. *Coord. Chem. Rev.* **1981**, *36*, 325.

(46) Oshawa, Y.; Hanck, K. W.; De Armond, M. K. *J. Electroanal. Chem.* **1984**, *175*, 229.

(47) Dodsworth, E. S.; Lever, A. B. P. *Chem. Phys. Lett.* **1986**, *124*, 152; *Ibid.* **1985**, *119*, 61; *Ibid.* **1984**, *112*, 567.

(48) Barigelletti, F.; Juris, A.; Balzani, V.; Belser, P.; von Zelewsky, A. *Inorg. Chem.* **1987**, *26*, 4115.

(49) Kawanishi, Y.; Kitamura, N.; Kim, Y.; Tazuke, S. *Sci. Pap. Inst. Phys. Chem. Res. (Jpn.)* **1984**, *78*, 212.

Table III. Kinetic Parameters for Radiative and Radiationless Decay in Nitrile Solution[a]

complex	$k^r \times 10^{-4}$,[b] s^{-1}	$k_0^{nr} \times 10^{-5}$,[c] s^{-1}	$B \times 10^{-5}$,[d] s^{-1}	A_e,[e] s^{-1}	ΔE_e,[e] cm^{-1}
1	6.7	1.4	2.0	1.3×10^{14}	3960
2	7.1	17.0	90		
3	6.0	4.7	14		
4	4.9	1.6	0.8	1.4×10^{10}	2760

[a] Estimated uncertainties on derived quantities are 20% on energies and 10% on ln (rate constants). [b] Radiative rate constant obtained from luminescence quantum yield and lifetime at 298 K, eq 6. [c] Nonradiative rate constant at 90 K, eq 3. [d] Increase in the nonradiative rate constant due to the melting of the solvent matrix (from eq 5). [e] Frequency factor and activation energy of the Arrhenius term describing the nonradiative process taking place at high temperature. For **3**, the numerical fitting gave $A_e = 2.5 \times 10^{+6}$ and $\Delta E_e = 15$ cm^{-1}.

$Ru(bpy)_3^{2+}$ (Table II). As mentioned above, in the cage complex the less electron-withdrawing amide groups replace the ester groups. Therefore, a displacement of the reduction potentials toward more positive values in going from **2** to **3** and **4** is expected and found (Table II). At first sight one would expect the first reduction potential of **4** to be very close to that of $Ru(bpy)_3^{2+}$, whereas the latter is 340 mV more negative. Again, solvation and, mainly, electronic effects should be responsible for the observed behavior.

Radiationless Transitions. The temperature dependence of the luminescence properties between 90 and 350 K has revealed important differences and similarities among the complexes examined. The plots of ln $(1/\tau)$ vs $1/T$ and of E_{max}^{em} vs $1/T$ are shown in Figures 4–6. For $Ru(bpy)_3^{2+}$ these plots have already been discussed[2,38] and are reported here for comparison purposes. To account for the temperature dependence of the luminescence lifetime of $Ru(bpy)_3^{2+}$ and several other coordination compounds,[2] $1/\tau$ can be expressed as a sum of a temperature-independent and several temperature-dependent terms:

$$1/\tau = k_0 + \sum_i k_i(T) \tag{2}$$

The temperature-independent term can be expressed by

$$k_0 = k^r + k_0^{nr} \tag{3}$$

where k^r is the radiative rate constant (usually taken to be temperature independent above 77 K[9,37,38]) and k_0^{nr} is a radiationless rate constant related to deactivation to the ground state via a weak-coupling mechanism. The temperature-dependent terms can be associated with radiationless processes related, in a schematic way, either to an activated surface crossing to another excited state, described by the Arrhenius equation

$$k_i^{nr} = A_i \exp(-\Delta E_i/RT) \tag{4}$$

or to the coming into play of effects (e.g., solvent repolarization) that do not occur at low temperature because of the frozen environment;[50-52] this second type of thermally activated process can be dealt with by the empirical equation[50]

$$k_i^{nr} = \frac{B_i}{1 + \exp[C_i(1/T - 1/T_{B_i})]} \tag{5}$$

which describes a stepwise change of lifetime centered at a certain temperature T_{B_i}. In eq 5, C_i is a temperature related to the smoothness of the step and B_i is the increment for k_i^{nr} at $T \gg T_{B_i}$. This equation is particularly useful to describe the behavior of a system in the glass–fluid region of a solvent matrix.[2] The radiative rate constant for the various complexes (Table III) can be obtained from the luminescence lifetime and luminescence quantum yield measured at room temperature (Table I):

$$k^r = \Phi_{em}/\tau \tag{6}$$

The values of k_0^{nr} can be obtained from the lifetime at 90 K, assuming that the radiative rate constant is temperature independent. According to the energy gap law,[53,54] a linear relationship is expected between ln k_0^{nr} and the spectroscopic energy, E^{00}, of the emitting level. Recent studies[54] have shown that for emission spectra of polypyridine-type complexes in rigid media $E_{max}^{em} = aE^{00} - b$, with $a \sim 1$ and b depending on the solvent and the complexes examined. Thus, a rough linear correlation is expected and is indeed observed between ln k_0^{nr} and E_{max}^{em} (90 K). In conclusion, the radiationless decays of the hemicaged **3** and caged **4** complexes at low temperature do not show any peculiar behavior with respect to the parent **1** and **2** complexes.

As one can see from Figure 5, in each case the ln $(1/\tau)$ vs $1/T$ plot exhibits a stepwise behavior in the temperature range corresponding to the melting of the solvent matrix (approximately 110–150 K). As is apparent from the figure, the additional k^{nr} term coming into play on solvent melting is relatively small for $Ru(bpy)_3^{2+}$ and **4**, much higher for **3**, and even higher for **2**. Equation 5 allows us to calculate such $k^{nr} = B$ terms that are collected in Table III. The very high B values for **2** and **3** can be associated with the fact that the light-induced MLCT extends to the peripherical ester groups, which are strongly sensitive to repolarization processes of the solvent environment, prevented in frozen matrix. $Ru(bpy)_3^{2+}$ and even more so the caged complex **4** are clearly less sensitive to the solvent, as shown by the smaller B values (Table III). The different sensitivities of the various complexes to the solvent are also shown by the shift of the emission maxima in the melting region. Figure 4 shows that for all complexes the melting of the solvent matrix causes a bathochromic shift of the emission band. As discussed previously, this shift is related to the solvent repolarization around the ^{3}MLCT excited state, which exhibits a different charge distribution with respect to the ground state because the promoted electron resides on the ligands. The shift shown by **4** is smaller than that of $Ru(bpy)_3^{2+}$ because the bridging groups present in the cage complex are not involved in the light-induced charge redistribution and are therefore expected to shield the chromophore from solvent interaction. Interestingly, at higher temperature ($T > 170$ K) the emission maxima of **2** and **3** show a hypsochromic shift (Figure 4), indicating a decrease in solvent polarization caused by thermal motions.

On increasing temperature above the solvent melting region, the plots of **2** and **3** show an almost temperature-independent behavior, whereas those for $Ru(bpy)_3^{2+}$ and **4** exhibit a further increase in ln $(1/\tau)$ (Figure 6), indicating that new radiationless pathways become available. For the latter complexes there is first a linear behavior of the ln $(1/\tau)$ vs $1/T$ plot, with a very small slope; then, at higher temperatures, the plot becomes much steeper, especially for $Ru(bpy)_3^{2+}$. The first portion of the plot can be accounted for in both cases by activation to a nearby MLCT level which exhibits a slightly higher k^{nr}. The steeper increase shown by the $Ru(bpy)_3^{2+}$ plot above 250 K can be accounted for by an Arrhenius term with high-frequency factor and large ΔE (Table III).[2,17,38,55-57] For **4**, the plot becomes smoothly steeper only above 300 K and the corresponding fequency factor and activation energy are both much smaller than those of $Ru(bpy)_3^{2+}$ (Table III).

For Ru(II)–polypyridine complexes the presence of an Arrhenius term

$$k_e = A_e \exp(-\Delta E_e/RT) \tag{7}$$

in the high-temperature region of the ln $(1/\tau)$ vs $1/T$ plots can

(50) Barigelletti, F.; Juris, A.; Balzani, V.; Belser, P.; von Zelewsky, A. *J. Phys. Chem.* **1987**, *91*, 1095.
(51) Kitamura, N.; Sato, M.; Kim, H.-B.; Obata, R.; Tazuke, S. *Inorg. Chem.* **1988**, *27*, 651.
(52) Danielson, E.; Lumpkin, R. S.; Meyer, T. J. *J. Phys. Chem.* **1987**, *91*, 1305.
(53) Engleman, R.; Jortner, J. *Mol. Phys.* **1970**, *18*, 145. Gelbart, W. M.; Freed, K. F.; Rice, S. A. *J. Chem. Phys.* **1970**, *52*, 2460. Robbins, D. J.; Thomson, A. J. *Mol. Phys.* **1973**, *25*, 1103.
(54) Caspar, J. V.; Meyer, T. J. *J. Am. Chem. Soc.* **1983**, *105*, 5583.
(55) Van Houten, J.; Watts, R. J. *J. Am. Chem. Soc.* **1976**, *98*, 4853.
(56) Meyer, T. J. *Pure Appl. Chem.* **1986**, *58*, 1193.
(57) Caspar, J. V.; Westmoreland, T. D.; Allen, G. H.; Bradley, P. G.; Meyer, T. J.; Woodruff, W. H. *J. Am. Chem. Soc.* **1984**, *106*, 3492.

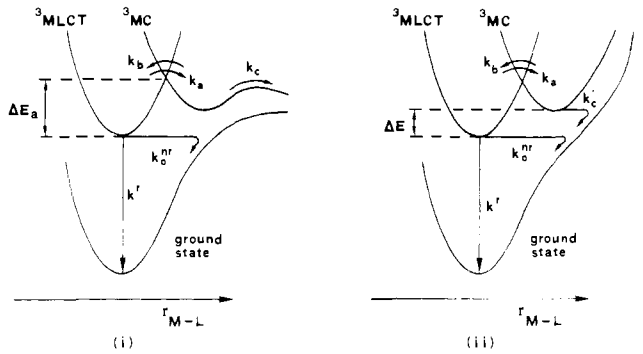

Figure 9. Schematic representation of two limiting cases for the situation of the potential energy surfaces. For more details, see text.

be associated with an activated surface crossing to an upper lying ^{3}MC excited state, which can then undergo fast deactivation to ground state and/or ligand dissociation products:[2,17,38,55-57]

$$^3\text{MLCT} \underset{k_b}{\overset{k_a}{\rightleftharpoons}} {}^3\text{MC} \qquad (8)$$

$$^3\text{MC} \xrightarrow{k_c} \text{ground state and/or photoproducts} \qquad (9)$$

Note that k_c represents the sum of all the rate constants of the processes that deactivate ^{3}MC, with the exception of the back-decay to ^{3}MLCT. The experimental deactivation rate constant that comes into play at high temperature (eq 7) can be expressed as follows on the basis of the mechanism given by eq 8 and 9:

$$k_e = k_a[k_c/(k_b + k_c)] \qquad (10)$$

As discussed in more detail elsewhere,[2] eq 10 can give rise to two limiting cases: (i) When $k_c \gg k_b$, the A_e and ΔE_e parameters obtained from the best fitting of the ln $(1/\tau)$ vs $1/T$ plots (Table III) correspond to the preexponential factor, A_a, and the activation energy, ΔE_a, for the ^{3}MLCT $\rightarrow$ ^{3}MC surface crossing, respectively (Figure 9i). (ii) When $k_b \gg k_c$, the meaning of the experimental quantities A_e and ΔE_e depends on the nature of the processes that contribute to k_c. When the main contribution to k_c comes from a nonactivated process, k'_c, the preexponential parameter A_e corresponds to the rate of the nonactivated ^{3}MC decay, k'_c, and the activation energy ΔE_e corresponds to the ^{3}MC - ^{3}MLCT energy gap, ΔE (Figure 9ii).

As previously pointed out,[2] it can be expected that A_a is a vibrational frequency (10^{13}–10^{14} s^{-1}) whose activation leads to surface crossing (Figure 9i). By contrast, k'_c can be much smaller because it represents the rate constant of radiationless transitions having a small Franck–Condon factor (Figure 9ii). $Ru(bpy)_3^{2+}$ ($A_e \sim 10^{14}$ s^{-1}, $\Delta E_e \sim 4000$ cm^{-1})[9] and several other Ru(II)–polypyridine complexes exhibiting comparable A_e and ΔE_e values are considered to belong to case i (Figure 9i). For **4**, the A_e value is too low to correspond to the frequency factor of a surface crossing process. Thus, we suggest that **4** corresponds to the limiting case described by Figure 9ii. The smaller ΔE_e value found for **4** compared with that of $Ru(bpy)_3^{2+}$ (Table III) is consistent with this hypothesis. Since the relative position of the ^{3}MLCT and ^{3}MC surfaces (near their minima) should be approximately the same in the two cases, ΔE_e should reflect the energy difference between the crossing point and the minimum of ^{3}MLCT for $Ru(bpy)_3^{2+}$ and the energy difference between the two minima for **4**, respectively (Figure 9i and ii).

The lack of temperature dependence of ln $(1/\tau)$ for **2** and **3** in fluid solution can be easily explained. For these complexes the energy gap between the ^{3}MC and ^{3}MLCT states is larger than that of **1** and **4** because of the lower energy of ^{3}MLCT. Thus, the Arrhenius term is expected to contribute to the radiationless decay only at higher temperatures. Furthermore, the higher values of B (Table III) would not allow the observation of activated processes having rate constants comparable to those observed for **1** and **4**.

Photochemical Behavior. As mentioned in the introduction, the ligand photodissociation reaction of $Ru(bpy)_3^{2+}$ is thought to proceed via the thermally activated radiationless transition, discussed in the previous section (Figure 9i), that leads from the ^{3}MLCT to the ^{3}MC state, with subsequent cleavage of one Ru–N bond and formation of an intermediate containing a monodentate bpy ligand.[2-5,16,17] Such an intermediate can then undergo either loss of bpy or chelate ring closure with reformation of $Ru(bpy)_3^{2+}$.[17]

The lack of ligand photodissociation for **2** and **3** can be easily explained on the basis of the temperature-dependence results discussed in the previous section. The ^{3}MC excited state is not accessible for these complexes because of the larger ^{3}MC – ^{3}MLCT energy gap and because of the faster radiationless decay of ^{3}MLCT directly to the ground state.[8-14]

The lack of ligand photodissociation for a caged complex is an expected result because there is no simple ligand to eject and the metal cannot easily escape the cage.[7,18,58] In the specific case of **4**, there can be at least three specific reasons for the observed photostability: (i) the ^{3}MC excited state is not populated; (ii) the ^{3}MC excited state cannot undergo ligand dissociation; (iii) if an intermediate containing a monodentate bpy ligand is formed, chelate ring closure regenerates the complex. We have seen above that $Ru(bpy)_3^{2+}$ and **4** exhibit quite similar spectroscopic properties and the energy gap between the ^{3}MLCT and ^{3}MC levels is expected to be approximately the same in the two complexes. Therefore, it is likely that the ^{3}MC level can be populated in the cage complex as it happens for $Ru(bpy)_3^{2+}$. The reason for the photostability of the cage complex must thus be found mainly in the prevention of strong nuclear distortions of ^{3}MC.

Quenching by Dioxygen. It is known that the quenching of the luminescent ^{3}MLCT excited state of $Ru(bpy)_3^{2+}$ by dioxygen in fluid solution takes place by an exchange energy transfer mechanism.[59-61] According to simple models, this mechanism requires overlap between pairs of orbitals exchanging two electrons.[62] Assuming that the dioxygen quenching of the ^{3}MLCT excited state of **4** takes place by the same mechanism, the 5 times lower value of the quenching constant compared to **1** (see Results) is not surprising, since the cage structure is expected to exert some shielding effect on the relevant orbitals of the complex.

It should also be noted that the alternative electron transfer quenching mechanism leading to the oxidized complex and O_2^-, which does not occur for $Ru(bpy)_3^{2+}$,[61] is even less favorable on thermodynamic grounds (Table II) for **4**.

Conclusions

When the bpy ligands of $Ru(bpy)_3^{2+}$ are linked together by suitable bridges, hemicaged **3** and caged **4** Ru(II) complexes are obtained that show quite interesting spectroscopic, photophysical, electrochemical, and photochemical properties. In particular, the cage complex **4** promises to be a better luminescent compound and a better photosensitizer than $Ru(bpy)_3^{2+}$ because it exhibits a quite similar absorption spectrum, practically the same excited-state energy, comparable redox properties, a longer excited-state lifetime at room temperature, and an approximately 10^4 times higher photochemical stability toward ligand release.

Acknowledgment. We wish to thank Mr. L. Minghetti and Mr. G. Gubellini for technical assistance. This work was supported by Progetto Strategico CNR "Reazioni di Trasferimento Monoelettronico", Ministero della Pubblica Istruzione (Italy), Swiss National Science Foundation, and Deutsche Forschungsgemeinschaft. F.E. is grateful to Fonds der Chemischen Industrie for a Kekulē stipend.

Registry No. **1**, 15158-62-0; **1**·$(PF_6)_2$, 60804-74-2; **2**, 74093-18-8; **2**·$(PF_6)_2$, 83605-48-5; **3**, 116952-00-2; **3**·$(PF_6)_2$, 120771-67-7; **4**, 116970-07-1; **4**·$(PF_6)_2$, 120771-68-8; O_2, 7782-44-7.

(58) Pina, F.; Ciano, M.; Moggi, L.; Balzani, V. *Inorg. Chem.* **1985**, *24*, 844.
(59) Demas, J. N.; Harris, E. W.; McBride, R. P. *J. Am. Chem. Soc.* **1977**, *99*, 3547.
(60) Demas, J. N.; McBride, R. P.; Harris, E. W. *J. Phys. Chem.* **1976**, *80*, 2248.
(61) Mulazzani, Q. G.; Ciano, M.; D'Angelantonio, M.; Venturi, M.; Rodgers, M. A. J. *J. Am. Chem. Soc.* **1988**, *110*, 2451.
(62) Kavarnos, G. J.; Turro, N. J. *Chem. Rev.* **1986**, *86*, 401.